

# Spatial patterns of phytoplankton communities in an International Seabed Authority licensed area (COMRA, Clarion-Clipperton Zone) in relation to upper ocean biogeochemistry

Yu Wang<sup>1†</sup>, Aiqin Han<sup>1†</sup>, Xuebao He<sup>1</sup>, Fangfang Kuang<sup>1</sup>, Feng Zhao<sup>2</sup>, Peng Xiang<sup>1\*</sup>, Kuidong Xu<sup>2\*</sup>

<sup>1</sup>Third Institute of Oceanography, Ministry of Natural Resources, Xiamen 361005, China

<sup>2</sup>Laboratory of Marine Organism Taxonomy and Phylogeny, Chinese Academy of Sciences, Qingdao 266071, China

Received 7 May 2021; accepted 21 June 2021

© Chinese Society for Oceanography and Springer-Verlag GmbH Germany, part of Springer Nature 2022

## Abstract

The Clarion-Clipperton Zone (CCZ) hosts one of the largest known oceanic nodule fields worldwide and is regulated by the International Seabed Authority. A baseline assessment of diversity and distribution patterns is essential for reliable predictions of disturbed ecosystem response scenarios for sustained commercial activities in the future. In the present study, the spatial patterns and diversity of phytoplankton communities were analyzed along with upper ocean biogeochemistry, in the licensed China Ocean Mineral Resources R&D Association (COMRA) contract area and the surrounding western CCZ between August 21 and October 8, 2017. Results indicated this was a typical low-nutrient low-chlorophyll *a* (Chl *a*) environment, characterized by low levels of phytoplankton abundance and diversity. In total 112 species belonging to 4 phyla were recorded (>10 μm), with species counts including 82 diatoms, 27 dinoflagellates, 1 cyanobacteria and 2 chrysophyte. Dominant taxa in successive order of descending abundance and occurrence included *Nitzschia marina*, *Cyclotella stylonum*, *Dactyliosolen mediterraneus*, *Rhizosolenia setigera*, *Pseudo-nitzschia delicatissima*, *Thalassiothrix frauenfeldii*, *Synedra* sp., *Chaetoceros simplex* and *Pseudo-nitzschia circumspora*. The depth-averaged abundance and Chl *a* concentrations were (265±233) cells/L and (0.27±0.30) μg/L, respectively. Diatoms accounted for 90.94% of the community with (241±223) cells/L, while dinoflagellates accounted for 5.67% and (15±13) cells/L. The distribution pattern exhibited the same trend as abundance, Chl *a* and species richness, showing subsurface maximum levels at around 100 m, with stations near 10°N having higher levels than in the north. Cluster analysis was performed in two assemblages, relating to geographic locations to the south and north of 12°N. The subsurface maximum of abundance, Chl *a*, species richness, dissolved oxygen and nitrite were generally corresponding to the presence of high salinity North Pacific Central Water at depths of 50–120 m. Higher availability of nitrate, phosphate and silicic acid in the subsurface may account for the shift in phytoplankton distribution, as shown by redundancy correspondence and spearman correlation analysis. Diel variation in an anchor station demonstrated prominent species succession without significant differences in oceanographic variables, among which diatoms succession resulted from the light limitation, while dinoflagellate diel variation mainly related to lateral transport of water masses. The observed patchiness in spatial phytoplankton distributional patterns was attributed to upper ocean environmental gradients in the CCZ. The baseline generated in this study could be analyzed using current conservation strategy programs associated with deep-sea mining.

**Key words:** phytoplankton communities, spatial patterns, diversity, upper ocean biogeochemistry, Clarion-Clipperton Zone, baseline assessment

**Citation:** Wang Yu, Han Aiqin, He Xuebao, Kuang Fangfang, Zhao Feng, Xiang Peng, Xu Kuidong. 2022. Spatial patterns of phytoplankton communities in an International Seabed Authority licensed area (COMRA, Clarion-Clipperton Zone) in relation to upper ocean biogeochemistry. Acta Oceanologica Sinica, 41(11): 45–57, doi: 10.1007/s13131-021-1938-4

## 1 Introduction

The offshore, subtropical Clarion-Clipperton Zone (CCZ), located in the eastern part of Pacific Ocean, southeastern part of Hawaii, is an area of interest for deep sea manganese nodule mining (International Seabed Authority (ISA), 2012; Dunn et al., 2018). Recent studies have demonstrated that mining activities in this region have serious negative environmental impacts, with post-disturbance recovery of the impacted ecosystem being an extremely long process, requiring a time range from decades to

potentially thousands of years (Jones et al., 2017; Kaiser et al., 2017). The ISA is responsible for the protection of marine environments from damage and overexploitation. To support this, much research has been undertaken in this region on marine organisms and the geological environment. Biodiversity from the deep sea to surface regions is of high importance, as polymetallic nodule ecosystems have been shown to host unique and largely unknown benthic communities (Vanreusel et al., 2016). A previous study on the polychaete fauna in the CCZ identified 183 spe-

Foundation item: The Project of Monitoring and Protection of Ecosystem in the East Pacific Ocean Sponsored by COMRA under contract No. DY135-E2-5-03; the National Natural Science Foundation of China under contract Nos 41506217 and 41506136; the Project of Ministry of Science and Technology under contract No. GASI-01-02-04.

\*Corresponding author, E-mail: xiangpeng@tio.org.cn; kxu@qdio.ac.cn

†These authors contributed equally to this work.

cies in an area of sea floor covering 19.25 m<sup>2</sup> (Glover et al., 2002). The species richness of the tanaidacean fauna associated with the CCZ has also been shown to be relatively high compared to other deep-sea tanaidacean studies with similar sampling methods (Błażewicz-Paszkwyc et al., 2015; Pabis et al., 2015). The high species richness of benthic fauna recorded in the CCZ might be due to the large scale of sampled area, as well as the high heterogeneity of the environment, which is primarily caused by the complex topography, the presence of natural barriers and differences in productivity among the license areas (Janssen et al., 2015; Zeppilli et al., 2016; Volz et al., 2018). Wilson et al. (2017) reported a decline in overall macrofauna and polychaete abundances from high and low productivity sites in the eastern equatorial Pacific. The observed latitudinal productivity gradient (particulate organic carbon flux; Vanreusel et al., 2016) in the CCZ was therefore reflected mainly in the sediment abiotic variables and only to a lesser extent in the faunal parameters. Productivity regimes in overlying waters dictate variability and a lack of homogeneity in assemblages of benthic meiofauna (Pape et al., 2013; Lins et al., 2014).

Phytoplankton are not only the most important primary producers in the marine ecosystem, but also play an important role in energy flow, material circulation and the transmission of information (Le Quéré et al., 2005). Changes in phytoplankton species composition, community structure and abundance, directly affect the water quality, energy flow, material flow and biological resources in ecosystems, having a direct effect on marine ecosystem stability (Finkel et al., 2010). Unfortunately, relatively little phytoplankton research has been undertaken in the CCZ region of the eastern Pacific Ocean. Zinssmeister et al. (2017) suggested that dinophysoid dinoflagellates species diversity was unexpectedly high in the eastern CCZ, with 66 taxa identified, along with novel species such as morphotypes being recorded. A study undertaken on Clipperton Island, a coral atoll in the northeastern Pacific Ocean at the eastern border of the CCZ, was described peridinoid dinoflagellate communities (Couté et al., 2012). A study was performed off the east coast of the US on the diversity of phytoplankton, recording 33 dinophysoid species within five genera (Kofoid and Skogsberg, 1928). However, to the best of our knowledge, the closest site to the CCZ investigated by phytoplankton taxonomists was around 850 km south-eastward, with the assessment undertaken a century ago (Marshall, 1976).

Therefore, the present study was undertaken to contribute to our understanding of phytoplankton (>10 µm) biodiversity in the

open eastern Pacific Ocean, especially in terms of the diversity of diatoms, dinoflagellates, cyanobacteria, chrysophyte and other species, with phytoplankton cell abundances and biomass quantified. Furthermore we explored the associations between biological patterns and major environmental variables.

## 2 Materials and methods

### 2.1 Study area and stations

The study area was the China mining claim (China Ocean Mineral Resources R&D Association (COMRA) contract area) located in the western CCZ. The COMRA contract area currently covers a total area of 75 000 km<sup>2</sup>, with an average depth of 5 200 m and ferromanganese nodule coverage of the ocean bed at an average density of 12 kg/m<sup>2</sup> (Shentu et al., 2009). The 8 sampling stations were located at 153°–156°W and between 8°N to 13°N in the COMRA contract area and the surrounding (Fig. 1). Among them, 4 stations (KW1-S37, KW1-S05, KW1-S40 and KW1-S01) were exactly in the COMRA contract area. To the north of COMRA contract area, 3 stations (CC-S06, CC-S09 and CC-S10) were selected and one station CC-S01 was set to its south. Furthermore, an anchor station KW1-S05 located at 10°N was visited at night time and in day time separately to demonstrate diel variation. Sampling was performed during the COMRA Cruise DY45 to the western part of the CCZ, along a north to south route between August 21 and October 8, 2017.

### 2.2 Sampling and determination

Temperature and salinity data were obtained using a SeaBird Electronics CTD system (SBE 911 plus, Florida), equipped with conductivity, temperature, depth and chlorophyll fluorescence probes. A Rosette hydrophore was used for the collection of water samples from depths of 5 m, 50 m, 75 m, 100 m, 150 m, 200 m and the subsurface chlorophyll maximum layer. Microscopy was performed on 2 L samples from each layer, with immediate fixing with Lugol's solution (final concentration 2%) after collection, followed by the addition of buffered formaldehyde (final concentration 2%) after 24 h. Once samples were returned to the laboratory, the collected phytoplankton samples were allowed to settle before being concentrated into a counting chamber. Cells were counted using the Utermöhl method and identified under a Zeiss Z1 inverted optical microscope at 200× or 400× magnification based on existing descriptions and taxonomic keys (Tomas, 1997; Sun and Liu, 2002; Guo and Qian, 2003). Abundances were calcu-

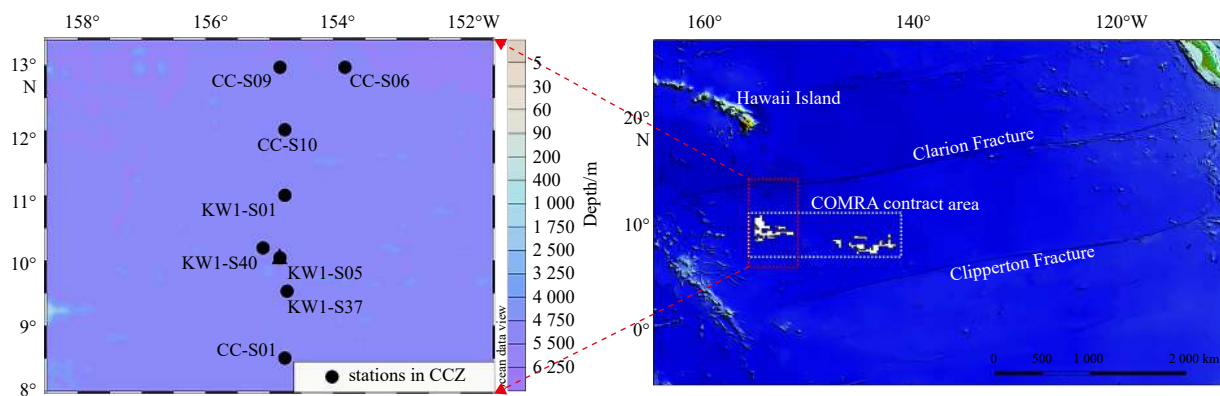


**Fig. 1.** The location and sampling stations of phytoplankton in the China Ocean Mineral Resources R&D Association (COMRA) contract area and the surrounding of western Clarion-Clipperton Zone (CCZ). KW1-S05 is an anchor station indicated in a triangle shape overlapping a dot.

lated for each species. Indistinguishable taxa were further characterized via electron scanning microscopy. Phytoplankton biomass was estimated using the chlorophyll *a* (Chl *a*) concentration as a proxy, established using a probe combined with CTD for the online real-time measurement of chlorophyll in vivo fluorescence.

Environmental variables were collected using Niskin water bottles and processed according to the methods described in *Specifications for Oceanographic Survey—Part 4: Survey of Chemical Parameters in Sea Water* (General Administration of Quality Supervision, Inspection and Quarantine of the People's Republic of China and Standardization Administration of China, 2008). Specifically, nitrate and nitrite concentrations were measured using the chemiluminescence method, at a detection limit of 0.1  $\mu\text{mol/L}$ . Ammonium was measured using the indophenol method, with a detection limit of 0.5  $\mu\text{mol/L}$ . Phosphorus was measured using the modified-MAGIC method with arsenate interference correction, with a detection limit of 0.05  $\mu\text{mol/L}$ . The silicon molybdenum blue spectrophotometric method was used for silicic acid, with a detection limit of 0.1  $\mu\text{mol/L}$ . The iodometric method was used to establish the oxygen concentration in water samples and the electrode potentiometric method was used to establish the pH. Suspended particulate matter (SPM) content was measured via the gravimetric method using a mixed fiber filter membrane with pore diameter of 0.45  $\mu\text{m}$  (General Administration of Quality Supervision, Inspection and Quarantine of the People's Republic of China and Standardization Administration of China, 2008).

Euphotic depth ( $Z_{\text{eu}}$ ) was obtained from the daily satellite dataset derived via ocean color remote sensing merged at 4 km on a spatial resolution from Globcolour (<http://hermes.acri.fr/>).

The satellite altimeter data of current velocity used was derived from satellites such as T/P, Jason and ERS1/2 provided by the AVISO (<http://www-aviso.cls.cnes.fr>). The quasi real-time data has been corrected for tides and sea surface pressures, with a spatial resolution of  $(1/3)^\circ$  and a time resolution of one day.

### 2.3 Statistical analysis

Data were analyzed by multivariate statistical methods. Logarithmic transformation [ $\log_{10}(x+1)$ ] was used to obtain a normal distribution of phytoplankton communities, with all environmental variable values transformed using  $\log_{10}(x)$ . Cluster analysis was used for community structure analysis (Primer 6 software). Detrended correspondence analysis was used for species data to determine which multivariate statistical methods would be applied (Canoco 5 software). Redundancy analysis (RDA) was used because the maximum gradient length of the four axes was less than three. Spearman's correlation coefficient was used to explore correlations between phytoplankton dynamics and oceanographic conditions (SPSS 17.0 software). Independent *t*-test was selected to evaluate fluctuations in phytoplankton community and oceanographic variables in the anchor station between night time and day time periods. Depth-averaged variables were calculated by dividing the trapezoidal integration of measured values for each variable by the maximum sampling depth.

## 3 Results

### 3.1 Oceanographic conditions

The temperature-salinity plot (Fig. 2) clearly shows four distinct water masses in the upper 200 m. Although the cores of the

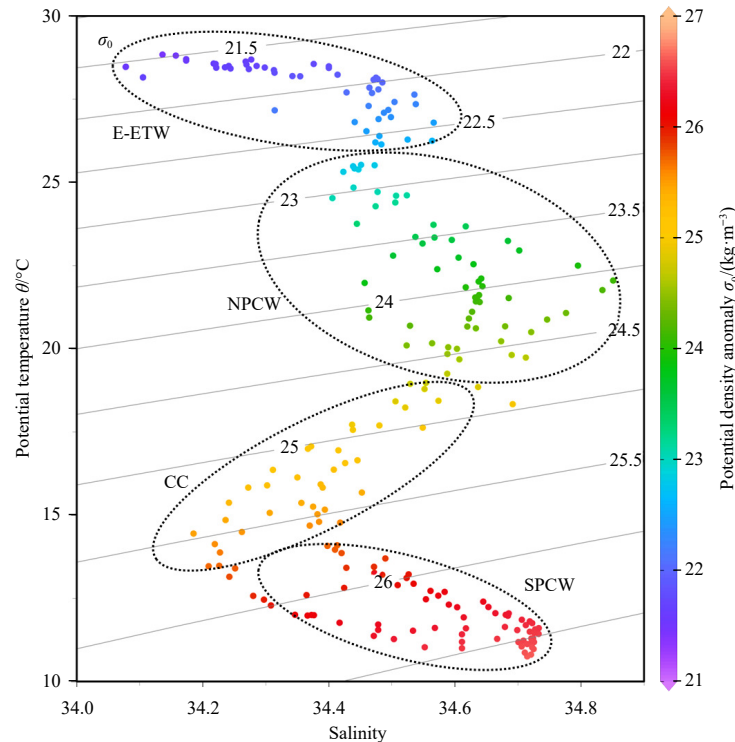


**Fig. 2.** Temperature-salinity diagram for given temperature and salinity data indicating characteristics of water masses in the China Ocean Mineral Resources R&D Association (COMRA) contract area and the surrounding of western Clarion-Clipperton Zone (CCZ). E-ETW: Eastern Equatorial Tropical Water; NPCW: North Pacific Central Water; CC: California Current; SPCW: South Pacific Central Water;  $\sigma_0$ : potential density anomaly.

water masses were clear, there were some differences observed among the subsurface water masses due to the wide latitudinal vertical span of nearly five latitudes (Fig. 3). The influence range of surface water was about 50 m, while the temperature of surface water was relatively uniform at an average of 27.8°C and the salinity ranged from 33.75–34.45. The water masses in subsurface depths of 50–120 m were located within the thermocline, with temperature and salinity ranges of 17.0–25.5°C and 34.50–

34.86, respectively. The salinity within the 50–120 m layer increased rapidly, exhibiting a gradually decreasing pattern from north to south. The salinity of water masses at subsurface depths of 120–180 m varied greatly from north to south. The salinity north of 12°N was <34.3, while south of 12°N it was relatively high, ranging from 34.4 to 34.5. The temperature in this region showed no significant difference, ranging from 12–17°C. The temperature of water masses at subsurface depths of 180–200 m slowly decre-

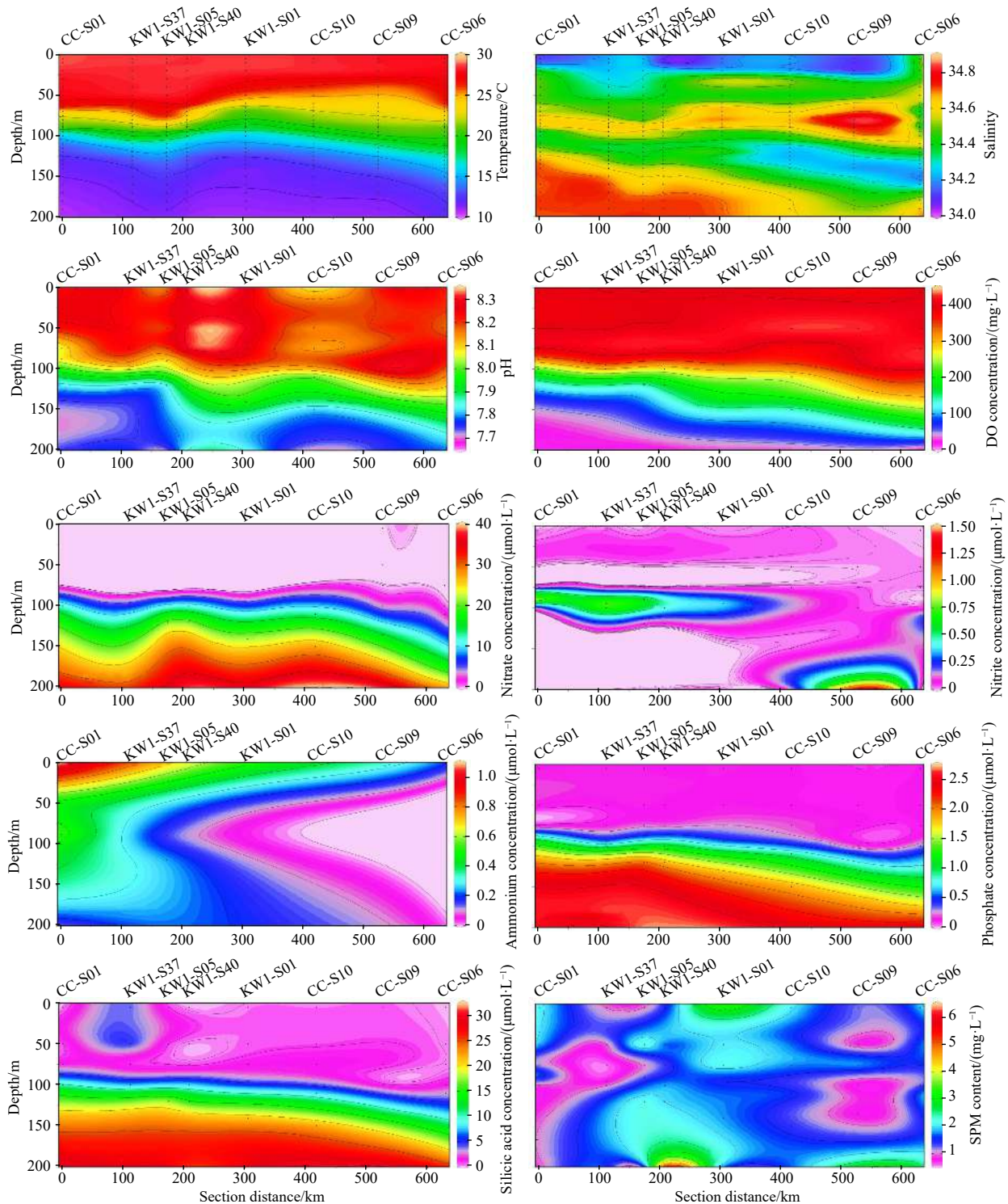


Fig. 3. Profile of oceanographic variables within 200 m in the China Ocean Mineral Resources R&D Association contract area and the surrounding of western Clarion-Clipperton Zone.

ased from 12°C to 9°C. Salinity increase compared with the adjacent upper water masses (120–180 m), ranging from 34.50 to 34.74, exhibiting a different distribution pattern to higher water masses, with an increase in salinity from north to south. In general, four distinct water masses were established from survey data from COMRA and its surrounding area from surface level to subsurface depths of 200 m, which were defined as Eastern Equatorial Tropical Water, North Pacific Central Water (NPCW), California Current and South Pacific Central Water (SPCW).

The assessed region was characterized as an oligotrophic ecosystem with low nutrient levels (Fig. 3). The phosphate concentrations in surface water were on average 0.16  $\mu\text{mol/L}$ , with an increased value of 0.52  $\mu\text{mol/L}$  observed from a depth of 80 m and reaching a maximum level at a depth of 200 m. Silicic acid concentrations were on average 1.10  $\mu\text{mol/L}$  at depths of above 50 m, with the vertical gradient varying greatly from 5 m to 80 m and then increasing at depths below 80 m. Nitrate concentrations above 80 m were <5  $\mu\text{mol/L}$  and increased consistently at greater depths, reaching a maximum level at 200 m. The nitrite concentrations above 50 m were generally <0.05  $\mu\text{mol/L}$ , showing large fluctuations between 50 m and 200 m. Maximum nitrite levels were located at subsurface depths of 80 m at Station KW1-S37 in the south and at depths of 200 m at Station CC-S09 in the north. Ammonium concentrations generally decreased according to depth, with highest concentrations mainly distributed in surface waters at Station CC-S01 in the south, while maximum levels gradually decreased to the north. The average pH was >8.1 from the surface to depth of 100 m and decreased at deeper level to 200 m. The DO concentration above 80 m was greater than 400  $\mu\text{mol/L}$ , decreasing with depth to reach a minimum level at 200 m. The maximum and minimum layers of DO were at the same depths as the maximum and minimum pH levels, respectively. The SPM content above 30 m was >1.6 mg/L, while its highest values were observed at a depth of 200 m at Stations KW1-S40 and CC-S09 in the north. In total, the spatial patchiness of temperature, salinity, pH and DO concentration were not as large as those found in nutrients and SPM content, but the overall trend of all variables distribution was diverse in the water column inventory from north to south.

At the anchor station, KW1-S05, the diel variability in observed oceanographic variables was non-significant (Table 1). Depth-averaged temperature and concentrations of phosphate,

**Table 1.** Independent *t*-test of oceanographic variables and phytoplankton abundance, Chl *a* concentration within 200 m between the two groups of night time and day time in the anchor station

Variable	Comparison between night time and day time periods
Temperature	$t=0.261, df=56, p=0.795$
Salinity	$t=-0.561, df=55.891, p=0.577$
pH	$t=0.664, df=10, p=0.535$
DO concentration	$t=0.147, df=10, p=0.886$
SPM content	$t=0.964, df=10, p=0.358$
Nitrate concentration	$t=-0.123, df=10, p=0.904$
Nitrite concentration	$t=-0.048, df=10, p=0.963$
Ammonium concentration	$t=0.064, df=9.894, p=0.951$
Phosphate concentration	$t=-0.050, df=10, p=0.961$
Silicic acid concentration	$t=-0.110, df=10, p=0.914$
Chl <i>a</i> concentration	$t=0.372, df=56, p=0.711$
Abundance	$t=0.680, df=10, p=0.512$

Note: The *df* means degree of freedom, which is a statistical term.

silicic acid and nitrate were higher during day time than night time. In contrast, all other variables were lower during the day time. Phosphate and silicic acid concentrations in particular, were much higher at depths below 100 m during day time, while salinity, DO concentration, pH and SPM content were greater at depths above 100 m during the night time (Fig. 4).

### 3.2 Chl *a* distribution

The depth-averaged Chl *a* concentration was  $(0.27\pm 0.30)$   $\mu\text{g/L}$ . In terms of profile distribution, Chl *a* fluorescence signal intensity in the southern region of the sampling area, especially at sites near 10°N, was slightly higher than in the northern region (Fig. 5). Generally, the maximum Chl *a* signal intensity was observed at subsurface depths of around 95 m. In the northern region, the subsurface Chl *a* maxima (SCM) at stations on a similar latitude were observed at greater depths (120 m) towards easterly longitudes.

Spatially, the depth-averaged Chl *a* maximum was observed at Station KW1-S05, at levels slightly higher than KW1-S01, while minimum concentrations were observed at Station CC-S09, which were 1.5-fold lower. At the anchor station KW1-S05, depth-averaged Chl *a* concentrations were evidently lower in the day time compared to at night, all of which were in the same order of magnitude, with maximum levels in both diel periods observed at 100 m. Chl *a* concentrations in upper depths to 100 m were lower in the day time than at night time, while at depths below 100 m the opposite trend was observed (Fig. 4).

### 3.3 Phytoplankton abundance distribution

The depth-averaged phytoplankton abundance was  $(265\pm 233)$  cells/L. Diatoms accounted for 90.94% of the community with  $(241\pm 223)$  cells/L, while dinoflagellates accounted for 5.67% with  $(15\pm 13)$  cells/L, cyanobacteria had an abundance of 2.77% with  $(10\pm 5)$  cells/L and the remaining species were chrysophyte. The distribution profile of abundances followed a similar pattern as the distribution of Chl *a*, with the southern sampling region exhibiting slightly higher abundances than the northern region (Fig. 6). Generally, the maximum abundances were observed at subsurface depths of about 100 m, with lower values observed at greater depths (130 m) to the north.

Spatially, the depth-averaged maximum abundance was observed at Station CC-S01, while the depth-averaged minimum abundance, which was about 4.4-fold lower, was observed at Station CC-S06. At the anchor station KW1-S05, the depth-averaged abundance at night time was marginally higher than during day time, although all values were in the same order of magnitude (Fig. 4). The diel variation in abundance in each water layer was relatively small, with the maximum abundances in both day time and night time observed at a depth of 100 m, while variation in abundances in the upper layer to depth of 100 m was larger in the day time than at night time (Fig. 4).

### 3.4 Community structure

A total of 4 phytoplankton phyla, 42 genera and 112 species (>10  $\mu\text{m}$ ) were recorded. In total, 82 diatom species were identified from 27 genera, 27 dinoflagellates species were found from 12 genera, while 1 cyanobacterial species and 2 chrysophyte species were observed. Diatoms were the main group found at all stations, contributing the most variability in terms of phytoplankton community species composition. In addition, diatoms were the most abundant species, with communities dominated by the genera *Chaetoceros* with 21 species recorded, *Rhizosolenia* with 7 species observed, *Nitzschia* and *Coscinodiscus* with 5 species

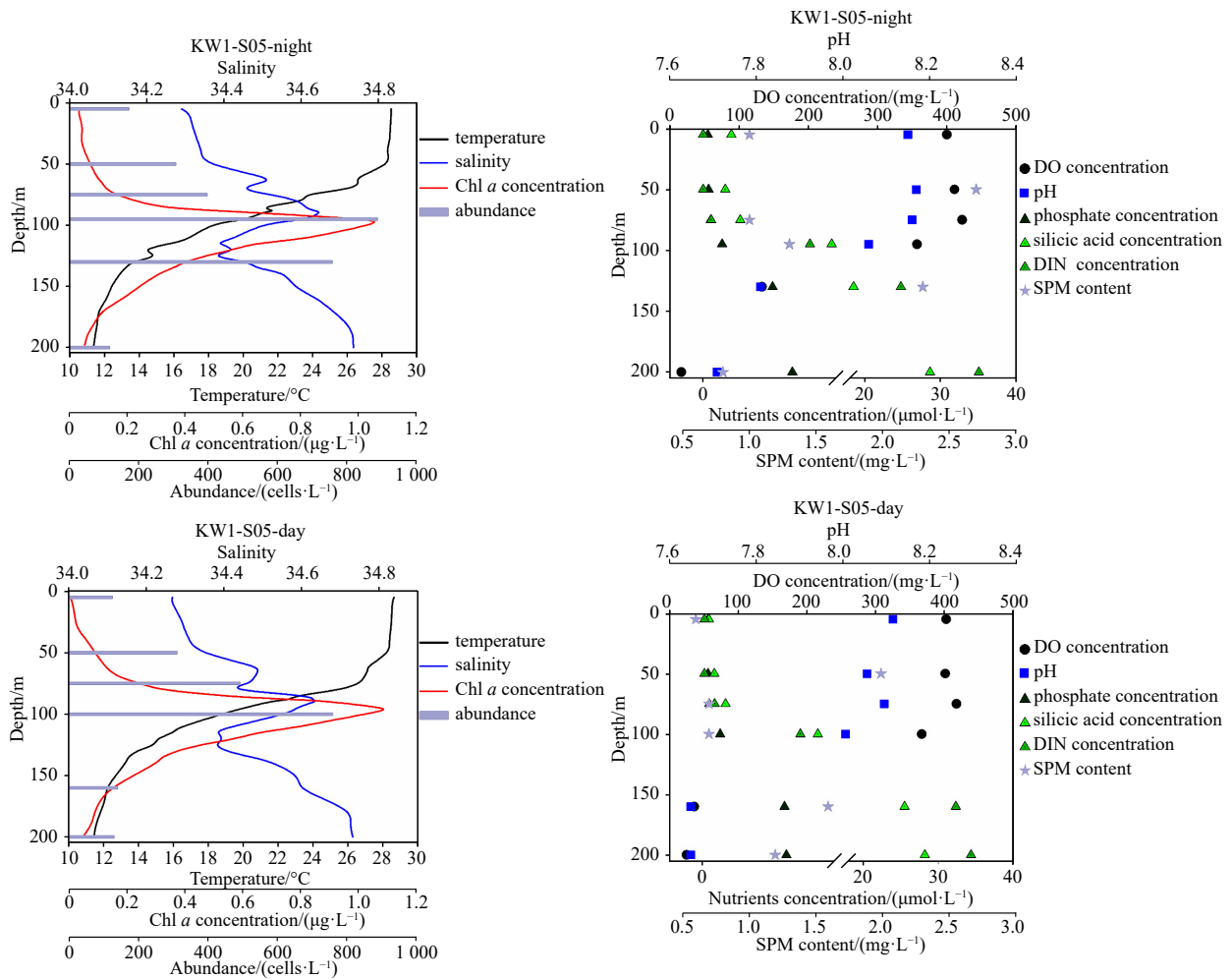


**Fig. 4.** Diel variations of oceanographic variables and phytoplankton abundance, Chl *a* concentration within 200 m in the anchor station between night time and day time.

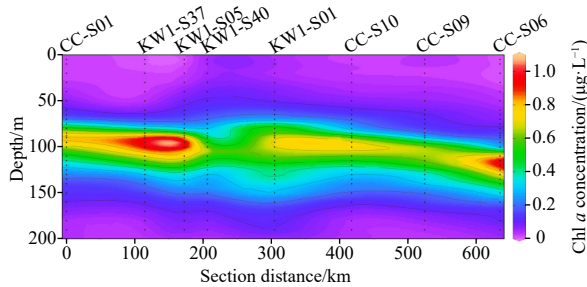


**Fig. 5.** Profile of phytoplankton Chl *a* ( $\mu\text{g/L}$ ) within 200 m in the China Ocean Mineral Resources R&D Association contract area and the surrounding of western Clarion-Clipperton Zone.

found for each. Dinoflagellates was also a major genera in the phytoplankton community, with 10 species of *Ceratium* and 3 species of *Amphidinium* and *Gyrodinium* each recorded. Spatially, the southern sampling region, especially at stations near  $9^{\circ}\text{N}$  and  $10^{\circ}\text{N}$ , exhibited a slightly higher level of species richness than the northern region above  $12^{\circ}\text{N}$  (Fig. 7). The maximum species richness was observed at depth of 120 m at Station KW1-S05 in the south, followed by Station CC-S01 at depth of 100 m. The minimum species richness was observed at a depth of 75 m in the north at the Station CC-S09 and at depth 5 m of Station CC-S10,

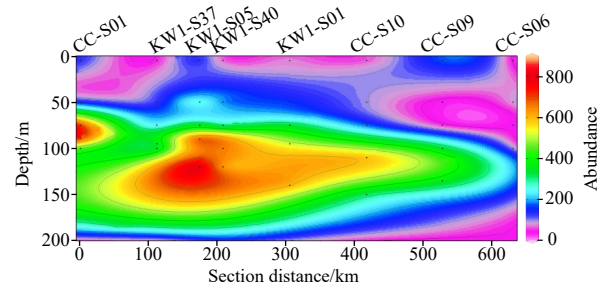


**Fig. 6.** Profile of phytoplankton abundance (cells/L) within 200 m in the China Ocean Mineral Resources R&D Association contract area and the surrounding of western Clarion-Clipperton Zone.

while in the south the minimum richness was observed at a depth of 5 m at Station CC-S01 (Fig. 7). Cyanobacteria were observed sporadically at depths below 75 m, mostly occurring at 100 m.

The dominant species were all diatoms, with abundance and occurrence ranked in the order of *Nitzschia marina*, *Cyclotella stylorum*, *Dactyliosolen mediterraneus*, *Rhizosolenia setigera*, *Pseudo-nitzschia delicatissima*, *Thalassiothrix frauenfeldii*, *Synedra* sp., *Chaetoceros simplex* and *Pseudo-nitzschia circumpora* (Table 2). Small *Cy. stylorum* and *N. marina* cells ( $<20\ \mu\text{m}$ ) had

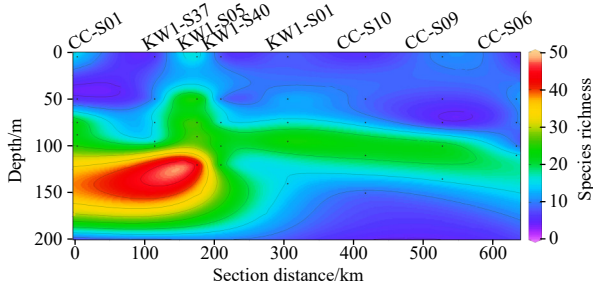


**Fig. 7.** Profile of phytoplankton species richness within 200 m in the China Ocean Mineral Resources R&D Association contract area and the surrounding of western Clarion-Clipperton Zone.

the greatest dominance at all sampling stations, followed by the warm-water adapted species *D. mediterraneus* and *R. setigera* (>100 μm). In contrast, the dominance of cosmopolitan *T. frauenfeldii* and *P. delicatissima* were low.

The anchor station KW1-S05 contained 48 species at night time and 44 species during day time. In total, 66 species were observed in both diel periods, among which 27 species were shared in both periods, accounting for 40.91% of the community, indicating that the night time and day time communities were significantly different with non-shared species reaching 59.09% (Fig. 8). The diel variation in dominant species was evident, with only *Ceratium teres* of dinoflagellates dominating in the day time, while the diatoms *Ch. simplex*, *R. setigera* and *T. frauenfeldii* were exclusively dominant at night time (Table 2).

Cluster analysis based on abundances among 75–150 m groups of phytoplankton indicated an assemblage to the south of 12°N due to the higher number of stations in this area and another assemblage to the north of 12°N including Stations CC-S09 and CC-S06 (Fig. 9). Some warm-water adapted species, such as *D. mediterraneus*, *R. setigera*, *Ch. simplex* and *P. circumpora*, existed in large abundances in the south assemblage, while only cosmopolitan species were highly abundant in the north assemblage, including *P. delicatissima*, *P. pungens* and *T. frauenfeldii*. In the south assemblage, the abundances of *T. longissima* and *P. circumpora* were much higher than in the north assemblage. Cluster analysis distinguished the stations at different latitudes, indicating that the observed biological pattern generally conformed to the surrounding environmental profiles in the

study area.

**3.5 Associations with oceanographic variables**

Correlations between phytoplankton species and oceanographic variables are shown in the biplot of RDA and Spearman correlation tests (Fig. 10, Table 3). Common phytoplankton species were mainly associated with the combination of phosphate and silicic acid, while nitrate was associated with the cosmopolitan species *Synedra* sp., *Nitzschia* spp. (including *N. marina*) and warm-water adapted *T. longissima*. Only cosmopolitan species *P. pungens* and *P. delicatissima* exhibited a preference according to pH and DO. *Rhizosolenia setigera* was found at greater abundances in warmer and nitrite-rich waters. Warm-water adapted *P. circumpora* and cosmopolitan *Cy. stylonum* also positively correlated with ammonium concentrations. Furthermore, there was a weak significant positive correlation between the abundance of certain diatom species and Chl *a* concentrations, due to the presence of low-nutrient low-Chl *a* (LNLC) condition.

Phytoplankton abundances and Chl *a* concentrations at depths from 5 m to 50 m were significantly positively correlated with nitrate concentrations, due to nitrogen depletion to non-detectable concentrations. Phosphate and silicic acid concentrations at depths from 50 m to 120 m were significantly positively correlated with phytoplankton abundance and Chl *a* concentration, while DO and pH were significantly negatively correlated. Both nitrate and nitrite were significantly positively correlated with phytoplankton abundance, while Chl *a* only exhibited a positive correlation with nitrite concentrations, while being negatively correlated with temperature. Both phytoplankton abundance and Chl *a* concentration were significantly positively correlated with temperature at depths of 120 m to 180 m. Salinity, phosphate and ammonium concentrations were significantly positively correlated with phytoplankton abundance at 200 m. Chl *a* concentration was positively associated to ammonium concentration.

**4 Discussion**

**4.1 Ecological features of phytoplankton communities in the COMRA contract area, CCZ**

The survey area was a typical LNLC environment, characterized by low nutrients and low phytoplankton abundance and diversity. The LNLC regions arise mainly due to large vertical strati-

**Table 2.** Dominant species in the whole region and its diel variation in the anchor station

Major taxa	A whole region			Anchor station-night time			Anchor station-day time		
	Contribution to total abundance	Occurrence frequent	Dominance	Contribution to total abundance	Occurrence frequent	Dominance	Contribution to total abundance	Occurrence frequent	Dominance
<i>Nitzschia marina</i>	0.123	0.889	0.109	0.042	1.000	0.042	0.046	1.000	0.046
<i>Cyclotella stylonum</i>	0.104	0.685	0.071	0.156	0.833	0.130	0.218	0.333	0.073
<i>Dactyliosolen mediterraneus</i>	0.053	0.463	0.025	0.044	0.500	0.022	0.056	0.500	0.028
<i>Rhizosolenia setigera</i>	0.065	0.352	0.023	0.130	0.667	0.087	0.010	0.167	0.002
<i>Pseudo-nitzschia delicatissima</i>	0.070	0.426	0.030	0.051	0.500	0.026	0.059	0.667	0.039
<i>Thalassiothrix frauenfeldii</i>	0.045	0.370	0.017	0.074	0.667	0.049	0.010	0.333	0.003
<i>Synedra</i> sp.	0.053	0.630	0.033	0.017	0.667	0.011	0.015	0.333	0.005
<i>Chaetoceros simplex</i>	0.033	0.389	0.013	0.065	0.833	0.054	0.005	0.333	0.002
<i>Pseudo-nitzschia circumpora</i>	0.040	0.167	0.007	0.021	0.500	0.011	0.146	0.167	0.024
<i>Nitzschia closterium</i>	0.026	0.296	0.008	0.027	0.333	0.009	0.010	0.333	0.003
<i>Thalassionema nitzschioides</i>	0.035	0.259	0.009	0.042	0.500	0.021	0.003	0.667	0.002
<i>Ceratium teres</i>	0.008	0.278	0.002	0.006	0.333	0.002	0.021	0.833	0.017

Note: The dominance is defined larger than 0.002 as the product of contribution and occurrence.

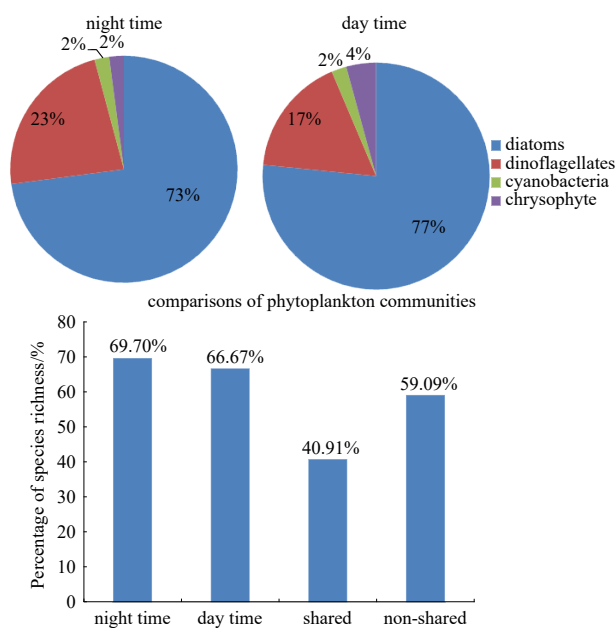


**Fig. 8.** Diel variation and comparisons of species richness occupations of shared and non-shared phytoplankton species between night time and day time in the anchor station KW1-S05.

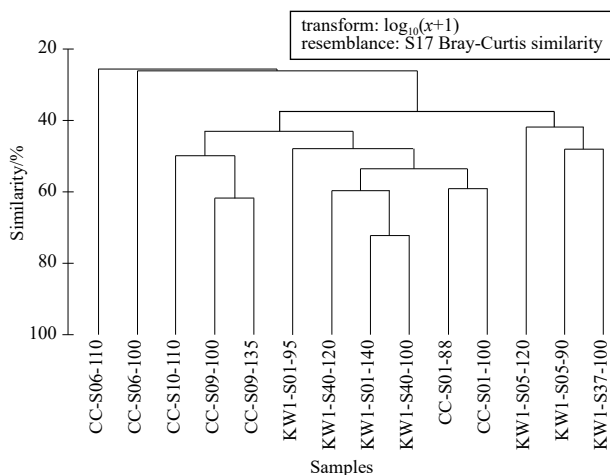


**Fig. 9.** Cluster analysis of phytoplankton assemblages associated to subsurface currents among 75–150 m in the China Ocean Mineral Resources R&D Association contract area and the surrounding of western Clarion-Clipperton Zone.

fication and a deep pycnocline generated by wind-forced anticyclonic subtropical gyres, which isolate the UV exposed, nutrient-depleted surface waters from the nutrient-rich waters below the euphotic zone (Karl and Letelier, 2008). SCM is a widespread feature in stratified oligotrophic oceans and is found in all but well-mixed waters (Cullen, 1982; Furuya and Marumo, 1983). The depth of the SCM is typically located at or near the depth of the nutricline, suggesting a compromise between nutrients supply from below and light from above (Johnson et al., 2010).

Generally, primary production and taxon-specific growth rates of phytoplankton showed no consistent temporal or spatial patterns or correlations with nutrient or Fe gradients in the eastern equatorial Pacific Ocean (Balch et al., 2011; Selph et al., 2011). In addition, Chl *a* concentrations, taxon-specific phytoplankton abundance and species richness in the COMRA west-

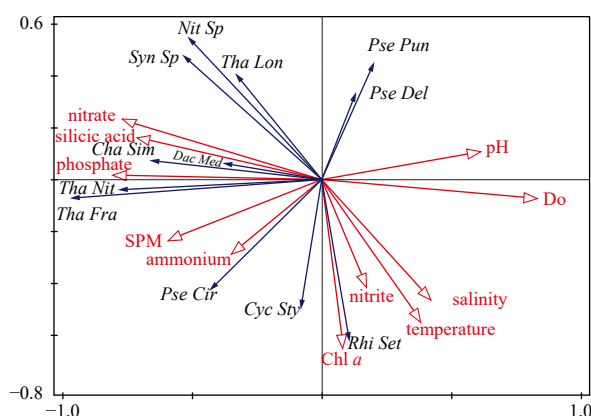


**Fig. 10.** Redundancy analysis of phytoplankton major species and oceanographic variables. Independent variables were temperature, salinity, pH, DO concentration, SPM content, nitrate concentration, nitrite concentration, ammonium concentration, phosphate concentration, silicic acid concentration and Chl *a* concentration. Biological variables include *Nit Sp*: *Nitzschia* sp., *Rhi Set*: *Rhizosolenia setigera*, *Pse Del*: *Pseudo-nitzschia delicatissima*, *Dac Med*: *Dactyliosolen mediterraneus*, *Syn Sp*: *Synedra* sp., *Tha Fra*: *Thalassionema frauenfeldii*, *Cyc Sty*: *Cyclotella stylonum*, *Cha Sim*: *Chaetoceros simplex*, *Tha Lon*: *Thalassiothrix longissima*, *Tha Nit*: *Thalassionema nitzschioides*, *Pse Cir*: *Pseudo-nitzschia circomphora*, *Pse Pun*: *Pseudo-nitzschia pungens*.

ern CCZ region, exhibited mainly consistent spatial patterns or correlations with DO distribution, salinity level and temperature gradients of water mass in the present study (Figs 3, 5–7), while similarities with the distribution pattern of nitrite gradients were only observed at depths between 75 m and 150 m (Figs 3, 5–7), which is in agreement with the results of previous reports in the eastern equatorial Pacific Ocean, indicating phytoplankton biomass and productivity varied only modestly with relative consistency (Selph et al., 2011; Taylor et al., 2011). In detail, the SCM (>0.5 mg/m<sup>3</sup>) occurred at depths between 90 m and 120 m, increasing to the north at higher latitudes. The maximum subsurface phytoplankton abundance (>700 cells/L) followed a similar pattern as Chl *a* concentrations, with differences only observed at depths of 100–130 m from south to north. Species richness at stations near 9°N and 10°N were higher than that in the north, with the highest richness mainly concentrated at depth of 100 m. Minimum DO concentrations (<0.5 μmol/L) were observed between 150 m and 200 m from southern to northern sampling regions. Therefore, the subsurface maximum Chl *a* concentration, phytoplankton abundance and spatial patchiness in species richness generally corresponded to the presence of high salinity NPCW at depths of 50–120 m, with a depth of 200 m exhibiting the lowest DO concentration associated with the high salinity SPCW.

The different depths of upper surface water among 200 m in the COMRA area were consistently found to be dominated by diatom species, along with one or two dominances of dinoflagellate species, although no dominant cyanobacteria were observed in upper layers. It has previously been observed that the abundance of cyanobacterial *Trichodesmium* populations is greater in the boundary current of the western Pacific Ocean (Capone et al., 1997), although this was not frequently observed in the western CCZ in the present study. Meanwhile, Zinssmeister et al. (2017) suggested that in the open waters of the eastern CCZ region, dinophysoids were one of the dominant taxa within the dinoflagellate community and among phytoplankton in general. However,

**Table 3.** Spearman correlation between phytoplankton abundance, Chl *a* concentration and oceanographic variables at each sampling layer

Depth	Variable	Temperature	Salinity	Nitrate concentration	Nitrite concentration	Ammonium concentration	Phosphate concentration	Silicic acid concentration	pH	DO concentration	SPM content	Chl <i>a</i> concentration
5–50 m	Chl <i>a</i> concentration	-0.474	0.315	1.000**	-0.387	-1.000**	0.006	0.004	0.324	0.394	0.242	-
	abundance	0.032	-0.052	-1.000**	-0.488	-1.000**	0.213	0.105	-0.012	-0.087	0.253	0.300
50–120 m	Chl <i>a</i> concentration	-0.538*	0.103	0.400	0.757**	-0.143	0.565**	0.622**	-0.492*	-0.618**	-0.169	-
	abundance	-0.409	-0.205	0.538*	0.495*	-0.086	0.578**	0.652**	-0.622**	-0.613**	0.184	0.493*
120–180 m	Chl <i>a</i> concentration	1.000**	0.500	-0.500	0.500	-	0.500	-0.500	0.500	0.500	0.500	-
	abundance	1.000**	0.500	-0.500	0.500	-	0.500	-0.500	0.500	0.500	0.500	1.000**
200 m	Chl <i>a</i> concentration	-0.048	0.119	-0.357	-0.071	1.000**	0.429	-0.190	0.119	-0.214	-0.527	-
	abundance	-0.060	0.826*	-0.108	-0.396	1.000**	0.946**	-0.575	0.395	-0.407	-0.223	0.252

Note: \*\* indicates  $p < 0.01$  (2-tailed); \*,  $p < 0.05$  (2-tailed); -, no data.

in the present study diatoms were found to be dominant in the phytoplankton community, followed by dinoflagellates, while cyanobacteria were seldom observed in any water samples from depths above 200 m in the western CCZ. The difference in results among these studies may be due to sampling method, as the previous results of Zinssmeister et al. (2017) were mainly based on net collected phytoplankton samples, while the present study assessed collected water samples. According to Hensen (1887) and Lohmann (1901), net collected phytoplankton samples are unable to capture all size ranges of phytoplankton in the water body, making it a semi quantitative method that can omit species smaller than the mesh size of the net. However, this method of net phytoplankton collection has certain advantages in oligotrophic oceans and allows direct comparison with historical data. For large phytoplankton (>100  $\mu\text{m}$ ) that can be captured using ordinary nets (commonly 76  $\mu\text{m}$  mesh size), the lost component due to net collection is not obvious (Sun et al., 2002). However, due to the large volume of sea water sampled during trawling, the species richness of collected phytoplankton is likely to be higher using net collection. Therefore, the species richness in dinophysoid of dinoflagellates (66 taxa) observed in the previous study is higher than the total species richness of dinoflagellate observed in the present study (27 taxa). In addition, the change in angle of inclination in the trawling process also affects the calculation to establish the volume of water column filtered (Sun et al., 2002), which can result in inaccuracies and imprecise quantitative trawling analysis results. Therefore, the abundance of phytoplankton may be underestimated by the influence of trawl mesh size and changes in trawl angle.

In the present study, diatoms exhibited obvious diel variability, which is supported by the results of previous studies (Stramski and Reynolds, 1993; Yang et al., 1994; van Haren et al., 1998; Tang and Chen, 2006; Bai et al., 2007). Dinoflagellates were documented vertical migration in day time and night time (Heaney and Eppley, 1981; Villarino et al., 1995). However, the dominance of dinoflagellates was not observed in day time or night time in this study, although an increase in large cell (>50  $\mu\text{m}$ ) dinoflagellate dominance of *Ceratium teres* was observed during the day time corresponding to the relatively high temperature and nutrients distributions (phosphate and silicic acid concentrations) (Fig. 4), which may be due to the strong lateral transport of water masses, resulting in a vertically stratified and stable water column inventory (e.g. Villarino et al., 1995; van Haren et al., 1998). Meanwhile, the lateral transport of water masses was prominent during the study period according to remote sensing. In the latitude of 12°–14°N, the average velocity was >40 cm/s, showing a stable westward direction. From 8°N to 11°N, the average velocity was about 30 cm/s flowing southward and eastward

(Fig. 11). While species such as chain-forming dinoflagellates, which are known to migrate vertically to gain access to resources (Raven and Richardson, 1984), have a selective advantage to survive in more turbulent water (Margalef et al., 1979; Fraga et al., 1989). However, the diel variation at the anchor station in this study was not exposed to such conditions and therefore, was dominated by diatoms both in day time and at night, primarily consisting of small cell (<20  $\mu\text{m}$ ) of *Cy. stylonum*, *N. marina* and *P. circumspora*.

#### 4.2 Controls on phytoplankton communities in the COMRA contract area, CCZ

The vast Pacific Ocean is not limited by the constraints of a land boundary and thus, water masses can move freely, including cross equatorial transport (Talley et al., 2011). In addition, condition dynamics such as the perennial stable trade wind in the tropical equatorial sea area, result in the overlapping distribution of the four water masses from top to bottom within 200 m of the investigated sea area (Tsuchiya, 1968; Kawai, 1972; Talley

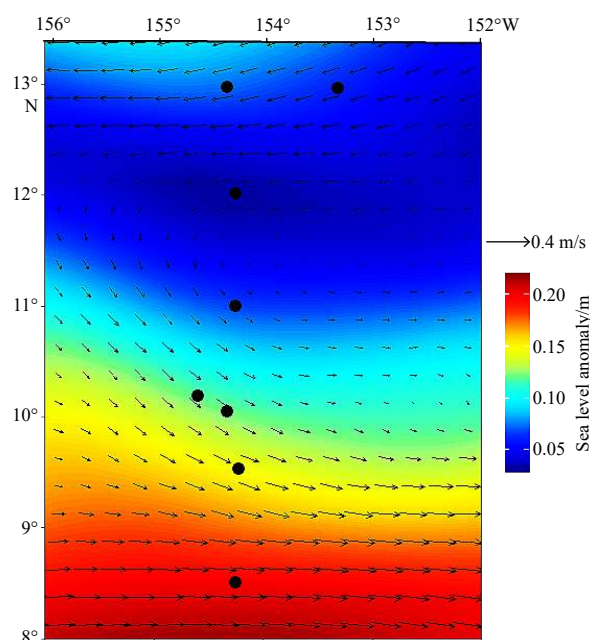


**Fig. 11.** The sea level anomaly (m) and geostrophic current velocity (m/s) in the western Clarion-Clipperton Zone (CCZ) from August 21 to October 8, 2017. Arrows indicated velocity and color bar indicated anomaly. Current velocity less than 0.4 m/s was not marked on the diagram. Black dots were station locations merged in the diagram.

et al., 2011). Previous results have shown that meridional migration of subsurface water masses occurs in the Pacific Ocean (Kawai, 1972; Talley et al., 2011). After the formation of NPCW in the subtropical convergence zone of 15°–30°N, which exhibits the highest level of salinity in the North Pacific Ocean, the NPCW then subsided and moved southward. During the southward migration, the NPCW began to increase, reached its highest level near 9°N with the 34.60 isohaline rose, at a depth of about 100 m (Talley et al., 2011). Therefore, in the study area, the NPCW controlled phytoplankton communities in the 50–120 m depth range. The latitudinal trend in subsurface maximum Chl *a* concentration, phytoplankton abundance, species richness and nitrite were largely associated with the NPCW. Furthermore, maximum DO levels gradually reduced from depths of 120 m to 80 m from 13°N to 8°N. Satellite data also showed that the  $Z_{eu}$  reduced at depths from 115 m to 100 m in accordance with a decrease in latitude during the study period in the western CCZ (Fig. 12). Therefore, the association of these variables spatial patterns under the NPCW regulation was evident.

The most direct impact of current on marine organisms is its role in spreading and maintaining biota. The transport of phytoplankton with current is well established, with some species migrating distances up to hundreds of kilometers (Darley, 1982; Huisman et al., 2002; Hallegraeff, 2010). The spatial patchiness in species richness among the sampling stations was prominent in the present study. Consistently, there were high occurrences of warm-water adapted species including *D. mediterraneus*, *R. setigera*, *R. alata*, *Ch. simplex* and *P. circumpora* in the southern region of the sampling area, especially at stations near 10°N (Stations KW1-S37 and KW1-S05). In contrast, cosmopolitan species such as *P. delicatissima*, *P. pungens* and *T. frauenfeldii* dominantly contributed to phytoplankton communities in the northern region, especially at stations beyond 12°N (Stations CC-S09 and CC-S06). Dupuis and Hann (2009) reported that sea surface temperature (SST) plays an essential role in controlling the physiology of plankton, which directly affects the community structure as plankton have been reported to have distinctive temperature ranges (Eppley, 1972). The maximum species richness was ob-

served slightly higher near 9°N and 10°N close to the equator, which may be due to increased insolation, warm temperature and the sufficient availability of nutrients (nitrite and ammonium concentrations) than in the northern region during this study (e.g., Richardson et al., 2000; Turner et al., 2009), for example SST was >28.50°C in the south of 10°N, maximum of nitrite and ammonium was found 0.989  $\mu\text{mol/L}$  and 1.05  $\mu\text{mol/L}$  near 9°N, respectively.

It is generally accepted that the diel variability in phytoplankton communities are related to tidal mixing, changes in nutrient content and feeding of zooplankton (Villarino et al., 1995; van Haren et al., 1998; Bai et al., 2007). During the night, the feeding pressure of zooplankton in the upper water layers is relatively high, resulting in phytoplankton biomass being relatively low (Gibbons, 1992; Cervetto et al., 1993). In addition, the vertical migration of dinoflagellates also leads to fluctuations in phytoplankton biomass (Villarino et al., 1995). In the present study, the dominant species were found to be diatoms and therefore, vertical migration cannot be the main reason for diel variations in phytoplankton distribution and abundance. The main reason for variability may be the reproduction or aggregation of diatom species (Stramski and Reynolds, 1993; van Haren et al., 1998; Jochem and Meyerdierks, 1999). In order to make full use of sunlight, it was previously speculated that the proliferation of unicellular species started during the day time, although it has now been proven that the diatom *Skeletonema* spp. initiates cell division at dawn (Jochem and Meyerdierks, 1999; Tang and Chen, 2006), showing that insolation plays a major role in phytoplankton growth. Moreover, another diatom *Thalassiosira gravida* was found the highest abundance around sunrise, and the lowest at night time (Stramski and Reynolds, 1993). In general, rates of dissolved silicic acid (DSi) uptake by diatoms diminished markedly with an increase in depth in the euphotic zone and were typically 3-fold higher in daylight hours than at night, suggesting DSi uptake is strongly dependent on ambient light intensity (Krause et al., 2011). Therefore, it was reasonable to imply diel variations in diatoms resulted from the light limitation, while dinoflagellate diel mainly related to lateral transport of water masses in the anchor station.

The nutrient status of seawater has a noticeable impact on the phytoplankton community structure. Criteria for stoichiometric nutrient limitation were developed based on nutrient requirements of diatoms. The atomic Si:N:P ratio of marine diatoms is about 16:16:1, when nutrient levels are sufficient (Redfield et al., 1963; Brzezinski, 1985). Deviations from this ratio either in nutrients taken up, or available in the water column is a dissolved form, indicate potential for N, P or Si limitation of phytoplankton growth (Hecky and Kilham, 1988; Dortch and Whitley, 1992). The concentrations of DSi (2  $\mu\text{mol/L}$ ), dissolved inorganic nitrogen (DIN, 1  $\mu\text{mol/L}$ ) and dissolved phosphate (0.1  $\mu\text{mol/L}$ ) were selected as threshold values (Fisher et al., 1992; Justić et al., 1995). Even though it has been debated about the general applicability of the classical Redfield ratio in the oceans (Koeve and Kähler, 2010; Martiny et al., 2013), the central tenet of Redfield's idea remains valid today (Gruber and Deutsch, 2014). Nitrogen globally limits marine primary productivity and bioavailable sources are mainly in the form of nitrate and ammonium (Falkowski, 1997). The western CCZ region and other oceans worldwide, are generally considered to be nitrogen-limited (<1.0  $\mu\text{mol/L}$ , threshold value) in euphotic zones. Hutchinson (1957) reported that oligotrophic waters exhibit higher nitrate concentrations due to the rapid nitrification process. Diatoms account for 12%–87% of the total nitrate uptake, with most estim-

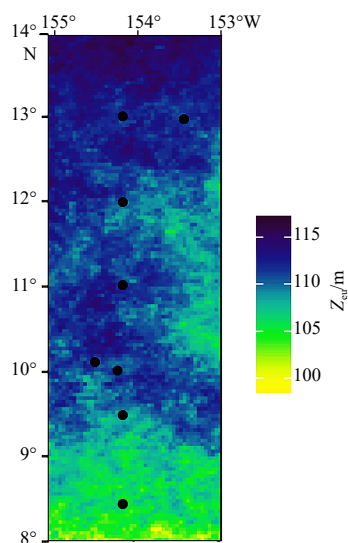


Fig. 12. Euphotic depth ( $Z_{eu}$ , m) in the western Clarion-Clipper-ton Zone from August 21 to October 8, 2017. Color bar indicated  $Z_{eu}$  depth derived via ocean color remote sensing. Black dots were station locations merged in the diagram.

ates being between 40% and 70% (Dugdale et al., 2011; Krause et al., 2011). Previous research found no clear relationship between nitrate uptake and calculated diatom nitrogen demand (Balch et al., 2011; Parker et al., 2011; Taylor et al., 2011). In the present study, nitrate concentrations were a strong driver for variation in the dominant diatom species and Chl *a* concentrations at depths above 50 m. The molar ratios of DIN/DIP (dissolved inorganic phosphorus) (1.15) and DIN/DSi (0.30) at depths of above 50 m were lower than the Redfield ratio (Redfield et al., 1963) and the typical uptake ratio for diatoms of 1:0.9 (Brzezinski et al., 2008). Among all sampling stations, nitrate depletion occurred where both phosphate and silicic acid concentrations were lower (Fig. 3). It is imperative to note that ammonium is a crucial nutrient along with nitrate, which is utilized by primary producers (Lipschultz, 1995), with nitrate being consumed while the concentration of ammonium reduced (Fang et al., 2008). However, ammonium was not found to be correlated with either diatom species or Chl *a* concentrations in the present study (Table 3). Moreover, nitrite was occasionally found to facilitate diatom species abundance and Chl *a* at depths of 50–120 m.

Phosphate availability is considered to be the proximal nutrient that limits primary production (Paytan and McLaughlin, 2007). Phytoplankton populations in tropical waters are mainly limited by phosphate concentrations (Cole and Sanford, 1989; Moutin et al., 2008). Many oligotrophic habitats seem to be particularly prone to severe phosphate limiting conditions (Karl, 2000). Stoecker (1999) found that phosphorus limitation was a common factor stimulating dinoflagellate ingestion of particulate nutrients. During this study, the average concentrations of nutrients at depths of 50 m to 120 m were found to be 6.08  $\mu\text{mol/L}$  (DIN), 0.62  $\mu\text{mol/L}$  (DIP) and 4.88  $\mu\text{mol/L}$  (silicic acid). The DIN was abundant and did not limit phytoplankton growth at depths between 50 m and 120 m. Therefore, the combination of phosphate and silicic acid becomes the limiting factor in the growth of phytoplankton. Furthermore, the average DSi/DIN molar ratio was 0.68 ( $<1$ , Redfield ratio), indicating a higher degree of limitation is induced by concentrations of silicic acid than nitrogen. In general, silicic acid significantly controls phytoplankton assemblages (Leblanc and Hutchins, 2005). It has previously been established that diatoms become dominant when silicic acid concentrations are  $>2 \mu\text{mol/L}$  (threshold value) and when other nutrient concentrations are sufficient (Fisher et al., 1992; Justić et al., 1995; Egge, 1998). As the average concentration of silicic acid was 28.5  $\mu\text{mol/L}$  at a depth of 200 m, with relative higher concentrations of phosphate (2.54  $\mu\text{mol/L}$ ) and DIN (35.4  $\mu\text{mol/L}$ ), diatoms could not be limited by silicic acid, indicating that phosphate may be the limiting factor in the growth of diatoms (Fisher et al., 1992; Egge, 1998; Ou et al., 2006). Overall, under the control of subsurface currents, phytoplankton community showed spatial patchiness associated with diverse oceanographic variables in the water column inventory from north to south in the COMRA contract area and the surrounding of western CCZ.

## 5 Conclusions

This study documented the phytoplankton community and its biomass distribution patterns within the upper 200 m of different geospatial locations in the western CCZ, revealing the relationship between phytoplankton and oceanographic variables. An important taxonomic study was successfully undertaken, to determine the diversity in phytoplankton communities, with 112 taxa identified and showing an overall domination by diatoms. Results from multivariate statistical analysis showed that phytoplankton communities exhibited significant differences between

the south and north of 12°N relating to geographical locations at different latitudes of oceanography in western CCZ. Phytoplankton distribution trends were generally consistent with trends in the surrounding oceanographic profiles in the study area. The subsurface maximum phytoplankton abundance, Chl *a* concentration, species richness and dissolved oxygen concentration corresponded to the presence of NPCW in the high salinity subsurface. Diel variations in diatoms resulted from the light limitation, while dinoflagellate diel mainly related to lateral transport of water masses. The study region generally was characterized as an open-ocean oligotrophic system with limited nutrient levels. Furthermore, phosphate and silicic acid were the most important environmental factors significantly correlated with phytoplankton communities.

Overall, the relatively low sampling coverage in this vast and poorly characterized ecosystem makes final conclusions on diversity, abundance and biomass highly uncertain. Nevertheless, the findings of previous studies have shown that polymetallic nodule mining in the CCZ region should be substantially delayed until the long-term ecological impacts can be adequately assessed (Vanreusel et al., 2016; Kaiser et al., 2017). Therefore, this baseline assessment of diversity and distribution patterns is essential for improved predictions and future development in this region. The data generated in this study should be analyzed using current conservation strategy programs associated with deep-sea mining (e.g. ISA, 2012; Dunn et al., 2018), with further extensive sampling also needed in the COMRA contract area. The complex interactions between phytoplankton and open-ocean characteristics need to be better explored with more detailed analysis, especially considering that the environmental consequences of deep-sea mining are still relatively poorly understood.

## Acknowledgements

The authors thank Senming Tang from Hongkong University for fruitful discussion and revising the manuscript; Hui Lin of Third Institute of Oceanography (TIO), Ministry of Natural Resources, for nutrients measurements; Weibo Wang of TIO for satellite data. We thank MogoEdit ([www.mogoedit.com](http://www.mogoedit.com)) for its linguistic assistance during the preparation of this manuscript. This work was also supported by COMRA and the R/V *Xiangyang 03* survey team.

## References

- Bai Jie, Jiang Yan, Sun Jun, et al. 2007. The diurnal fluctuation of phytoplankton vertical distribution adjacent to the Yellow Sea cold water mass. *Periodical of Ocean University of China*, 37(6): 1013–1016, 938
- Balch W M, Poulton A J, Drapeau D T, et al. 2011. Zonal and meridional patterns of phytoplankton biomass and carbon fixation in the equatorial Pacific Ocean, between 110°W and 140°W. *Deep-Sea Research Part II: Topical Studies in Oceanography*, 58(3–4): 400–416
- Błażewicz-Paszkwowycz M, Pabis K, Józwiak P. 2015. Tanaidacean fauna of the Kuril-Kamchatka Trench and adjacent abyssal plain-abundance, diversity and rare species. *Deep-Sea Research Part II: Topical Studies in Oceanography*, 111: 325–332, doi: 10.1016/j.dsr2.2014.08.021
- Brzezinski M A. 1985. The Si: C: N ratio of marine diatoms: interspecific variability and the effect of some environmental variables. *Journal of Phycology*, 21(3): 347–357
- Brzezinski M A, Dumousséaud C, Krause J W, et al. 2008. Iron and silicic acid concentrations together regulate Si uptake in the equatorial Pacific Ocean. *Limnology and Oceanography*, 53(3): 875–889, doi: 10.4319/lo.2008.53.3.0875
- Capone D G, Zehr J P, Paerl H W, et al. 1997. *Trichodesmium*, a glob-

- ally significant marine cyanobacterium. *Science*, 276(5316): 1221–1229, doi: [10.1126/science.276.5316.1221](https://doi.org/10.1126/science.276.5316.1221)
- Cervetto G, Gaudy R, Pagano M, et al. 1993. Diel variations in *Acartia tonsa* feeding, respiration and egg production in a Mediterranean coastal lagoon. *Journal of Plankton Research*, 15(11): 1207–1228, doi: [10.1093/plankt/15.11.1207](https://doi.org/10.1093/plankt/15.11.1207)
- Cole C V, Sanford R L. 1989. Biological aspects of the phosphorus cycle. In: Proceedings Symposium on Phosphorous Requirements for Sustainable Agriculture in Asia and Oceania. Los Banos, Philippines: International Rice Research Institute
- Couté A, Perrette C, Chomérat N. 2012. Three Dinophyceae from Clipperton Island lagoon (eastern Pacific Ocean), including a description of *Peridiniopsis cristata* var. *tubulifera* var. nov. *Botanica Marina*, 55(1): 59–71, doi: [10.1515/bot-2011-121](https://doi.org/10.1515/bot-2011-121)
- Cullen J J. 1982. The deep chlorophyll maximum: comparing vertical profiles of chlorophyll *a*. *Canadian Journal of Fisheries and Aquatic Sciences*, 39(5): 791–803, doi: [10.1139/f82-108](https://doi.org/10.1139/f82-108)
- Darley W M. 1982. *Algal Biology: A Physiological Approach*. Oxford: Blackwell Scientific Publications, 168
- Dortch Q, Whitedge T E. 1992. Does nitrogen or silicon limit phytoplankton production in the Mississippi River plume and nearby regions?. *Continental Shelf Research*, 12(11): 1293–1309, doi: [10.1016/0278-4343\(92\)90065-R](https://doi.org/10.1016/0278-4343(92)90065-R)
- Dugdale R C, Chai Fei, Feely R A, et al. 2011. The regulation of equatorial Pacific new production and pCO<sub>2</sub> by silicate-limited diatoms. *Deep-Sea Research Part II: Topical Studies in Oceanography*, 58(3–4): 477–492
- Dunn D C, van Dover C L, Etter R J, et al. 2018. A strategy for the conservation of biodiversity on mid-ocean ridges from deep-sea mining. *Science Advances*, 4(7): eaar4313, doi: [10.1126/sciadv.aar4313](https://doi.org/10.1126/sciadv.aar4313)
- Dupuis A P, Hann B J. 2009. Warm spring and summer water temperatures in small eutrophic lakes of the Canadian prairies: potential implications for phytoplankton and zooplankton. *Journal of Plankton Research*, 31(5): 489–502, doi: [10.1093/plankt/fbp001](https://doi.org/10.1093/plankt/fbp001)
- EGGE J K. 1998. Are diatoms poor competitors at low phosphate concentrations?. *Journal of Marine Systems*, 16(3–4): 191–198
- Eppley R W. 1972. Temperature and phytoplankton growth in the sea. *Fishery Bulletin*, 70(4): 1063–1085
- Falkowski P G. 1997. Evolution of the nitrogen cycle and its influence on the biological sequestration of CO<sub>2</sub> in the ocean. *Nature*, 387(6630): 272–275, doi: [10.1038/387272a0](https://doi.org/10.1038/387272a0)
- Fang Tao, Li Daoji, Yu Lihua, et al. 2008. Changes in nutrient uptake of phytoplankton under the interaction between sunlight and phosphate in the Changjiang (Yangtze) River Estuary. *Chinese Journal of Geochemistry*, 27(2): 161–170, doi: [10.1007/s11631-008-0161-8](https://doi.org/10.1007/s11631-008-0161-8)
- Finkel Z V, Beardall J, Flynn K J, et al. 2010. Phytoplankton in a changing world: cell size and elemental stoichiometry. *Journal of Plankton Research*, 32(1): 119–137, doi: [10.1093/plankt/fbp098](https://doi.org/10.1093/plankt/fbp098)
- Fisher T R, Peele E R, Ammerman J W, et al. 1992. Nutrient limitation of phytoplankton in Chesapeake Bay. *Marine Ecology Progress Series*, 82: 51–63, doi: [10.3354/meps082051](https://doi.org/10.3354/meps082051)
- Fraga S, Gallagher S M, Anderson D M. 1989. Chain-forming dinoflagellates: an adaptation to red tides. In: Okaichi T, Anderson D M, Nemoto T, eds. *Red Tides: Biology, Environmental Science and Toxicology*. Amsterdam: Elsevier, 281–284
- Furuya K, Marumo R. 1983. The structure of the phytoplankton community in the subsurface chlorophyll maxima in the western North Pacific Ocean. *Journal of Plankton Research*, 5(3): 393–406, doi: [10.1093/plankt/5.3.393](https://doi.org/10.1093/plankt/5.3.393)
- General Administration of Quality Supervision, Inspection and Quarantine of the People's Republic of China, Standardization Administration of China. 2008. GB/T 12763.4–2007. Specifications for Oceanographic Survey—Part 4: Survey of Chemical Parameters in Sea Water. Beijing: Standards Press of China, 1–65
- Gibbons M J. 1992. Diel feeding and vertical migration of *Sagitta serratodentata* Krohn *tasmanica* Thomson (Chaetognatha) in the southern Benguela. *Journal of Plankton Research*, 14(2): 249–259, doi: [10.1093/plankt/14.2.249](https://doi.org/10.1093/plankt/14.2.249)
- Glover A G, Smith C R, Paterson G L J, et al. 2002. Polychaete species diversity in the central Pacific abyss: local and regional patterns, and relationships with productivity. *Marine Ecology Progress Series*, 240: 157–170, doi: [10.3354/meps240157](https://doi.org/10.3354/meps240157)
- Gruber N, Deutsch C A. 2014. Redfield's evolving legacy. *Nature Geoscience*, 7(12): 853–855, doi: [10.1038/ngeo2308](https://doi.org/10.1038/ngeo2308)
- Guo Yujie, Qian Shuben. 2003. *China Sea-weed Records: Fifth Volume Bacillariophyta*. Beijing: Science Press. 1–493
- Hallegraeff G M. 2010. Ocean climate change, phytoplankton community responses, and harmful algal blooms: a formidable predictive challenge. *Journal of Phycology*, 46(2): 220–235, doi: [10.1111/j.1529-8817.2010.00815.x](https://doi.org/10.1111/j.1529-8817.2010.00815.x)
- Heaney S I, Eppley R W. 1981. Light, temperature and nitrogen as interacting factors affecting diel vertical migrations of dinoflagellates in culture. *Journal of Plankton Research*, 3(2): 331–344, doi: [10.1093/plankt/3.2.331](https://doi.org/10.1093/plankt/3.2.331)
- Hecky R E, Kilham P. 1988. Nutrient limitation of phytoplankton in freshwater and marine environments: a review of recent evidence on the effects of enrichment. *Limnology and Oceanography*, 33(4part2): 796–822, doi: [10.4319/lo.1988.33.4part2.0796](https://doi.org/10.4319/lo.1988.33.4part2.0796)
- Hensen V. 1887. über die Bestimmung des Planktonsoder des Meeretreibenden Materials an Pflanzen und Thieren. Kommission zur wissenschaftlichen Untersuchung der deutschen Meere in Kiel: 1882–1886. V Bericht Jahrgang (in German), 12–16: 1–107
- Huisman J, Arrayás M, Ebert U, et al. 2002. How do sinking phytoplankton species manage to persist?. *The American Naturalist*, 159(3): 245–254, doi: [10.1086/338511](https://doi.org/10.1086/338511)
- Hutchinson G E. 1957. Concluding remarks. *Cold Spring Harbor Symposia on Quantitative Biology*, 22: 415–427, doi: [10.1101/SQB.1957.022.01.039](https://doi.org/10.1101/SQB.1957.022.01.039)
- International Seabed Authority (ISA). 2012. Decision of the Council relating to an environmental management plan for the Clarion-Clipperton Zone. ISBA/18/C/22. Kingston, Jamaica: International Seabed Authority
- Janssen A, Kaiser S, Meißner K, et al. 2015. A reverse taxonomic approach to assess macrofaunal distribution patterns in abyssal Pacific polymetallic nodule fields. *PLoS ONE*, 10(2): e0117790, doi: [10.1371/journal.pone.0117790](https://doi.org/10.1371/journal.pone.0117790)
- Jochem F J, Meyerdierks D. 1999. Cytometric measurement of the DNA cell cycle in the presence of chlorophyll autofluorescence in marine eukaryotic phytoplankton by the blue-light excited dye YOYO-1. *Marine Ecology Progress Series*, 185: 301–307, doi: [10.3354/meps185301](https://doi.org/10.3354/meps185301)
- Johnson Z I, Shyam R, Ritchie A E, et al. 2010. The effect of iron- and light-limitation on phytoplankton communities of deep chlorophyll maxima of the western Pacific Ocean. *Journal of Marine Research*, 68(2): 283–308, doi: [10.1357/002224010793721433](https://doi.org/10.1357/002224010793721433)
- Jones D O B, Kaiser S, Sweetman A K, et al. 2017. Biological responses to disturbance from simulated deep-sea polymetallic nodule mining. *PLoS ONE*, 12(2): e0171750, doi: [10.1371/journal.pone.0171750](https://doi.org/10.1371/journal.pone.0171750)
- Juštíć D, Rabalais N N, Turner R E, et al. 1995. Changes in nutrient structure of river-dominated coastal waters: stoichiometric nutrient balance and its consequences. *Estuarine, Coastal and Shelf Science*, 40(3): 339–356
- Kaiser S, Smith C R, Arbizu P M. 2017. Editorial: biodiversity of the Clarion Clipperton Fracture Zone. *Marine Biodiversity*, 47(2): 259–264, doi: [10.1007/s12526-017-0733-0](https://doi.org/10.1007/s12526-017-0733-0)
- Karl D M. 2000. Phosphorus, the staff of life. *Nature*, 406(6791): 31–33
- Karl D M, Letelier R M. 2008. Nitrogen fixation-enhanced carbon sequestration in low nitrate, low chlorophyll seascapes. *Marine Ecology Progress Series*, 364: 257–268, doi: [10.3354/meps07547](https://doi.org/10.3354/meps07547)
- Kawai H. 1972. Hydrography of the Kuroshio Extension. In: Stommel H, Yoshida K, eds. *Kuroshio, Its Physical Aspects*. Tokyo: University of Tokyo Press, 235–352
- Koeve W, Kähler P. 2010. Balancing ocean nitrogen. *Nature Geoscience*, 3(6): 383–384, doi: [10.1038/ngeo884](https://doi.org/10.1038/ngeo884)
- Kofoed C A, Skogsberg T. 1928. *The Dinoflagellata: the Dinophysoidae*. *Memoirs of the Museum of Comparative Zoology*, 51: 1–766
- Krause J W, Nelson D M, Brzezinski M A. 2011. Biogenic silica pro-

- duction and the diatom contribution to primary production and nitrate uptake in the eastern equatorial Pacific Ocean. *Deep-Sea Research Part II: Topical Studies in Oceanography*, 58(3–4): 434–448
- Le Quéré C, Harrison S P, Prentice I C, et al. 2005. Ecosystem dynamics based on plankton functional types for global ocean biogeochemistry models. *Global Change Biology*, 11(11): 2016–2040
- Leblanc K, Hutchins D A. 2005. New applications of a biogenic silica deposition fluorophore in the study of oceanic diatoms. *Limnology and Oceanography: Methods*, 3(10): 462–476, doi: [10.4319/lom.2005.3.462](https://doi.org/10.4319/lom.2005.3.462)
- Lins L, Guilini K, Veit-Köhler G, et al. 2014. The link between meiofauna and surface productivity in the Southern Ocean. *Deep-Sea Research Part II: Topical Studies in Oceanography*, 108: 60–68, doi: [10.1016/j.dsr2.2014.05.003](https://doi.org/10.1016/j.dsr2.2014.05.003)
- Lipschultz F. 1995. Nitrogen-specific uptake rates of marine phytoplankton isolated from natural populations of particles by flow cytometry. *Marine Ecology Progress Series*, 123: 245–258, doi: [10.3354/meps123245](https://doi.org/10.3354/meps123245)
- Lohmann H. 1901. Ueber das Fischen mit Netzen aus Müllergaze No 20. *Wissenschaftliche Meeresuntersuchungen Abth. Kiel. (Neue Folge)*, 5: 45–66
- Margalef R, Estrada M, Blasco D. 1979. Functional morphology of organisms involved in red tides, as adapted to decaying turbulence. In: Taylor D L, Seliger H H, eds. *Toxic Dinoflagellate Blooms*. New York: Elsevier, 89–94
- Marshall H G. 1976. Phytoplankton distribution along the eastern coast of the USA. I. Phytoplankton composition. *Marine Biology*, 38(1): 81–89, doi: [10.1007/BF00391488](https://doi.org/10.1007/BF00391488)
- Martiny A C, Pham C T A, Primeau F W, et al. 2013. Strong latitudinal patterns in the elemental ratios of marine plankton and organic matter. *Nature Geoscience*, 6(4): 279–283, doi: [10.1038/ngeo1757](https://doi.org/10.1038/ngeo1757)
- Moutin T, Karl D M, Duhamel S, et al. 2008. Phosphate availability and the ultimate control of new nitrogen input by nitrogen fixation in the tropical Pacific Ocean. *Biogeosciences*, 5(1): 95–109, doi: [10.5194/bg-5-95-2008](https://doi.org/10.5194/bg-5-95-2008)
- Ou Linjian, Huang Bangqin, Lin Lizhen, et al. 2006. Phosphorus stress of phytoplankton in the Taiwan Strait determined by bulk and single-cell alkaline phosphatase activity assays. *Marine Ecology Progress Series*, 327: 95–106, doi: [10.3354/meps327095](https://doi.org/10.3354/meps327095)
- Pabis K, Błażewicz-Paszkowycz M, Józwiak P, et al. 2015. Tanaidacea of the Amundsen and Scotia Seas: an unexplored diversity. *Antarctic Science*, 27(1): 19–30, doi: [10.1017/S0954102014000303](https://doi.org/10.1017/S0954102014000303)
- Pape E, Jones D O B, Manini E, et al. 2013. Benthic-pelagic coupling: effects on nematode communities along southern European continental margins. *PLoS ONE*, 8(4): e59954, doi: [10.1371/journal.pone.0059954](https://doi.org/10.1371/journal.pone.0059954)
- Parker A E, Wilkerson F P, Dugdale R C, et al. 2011. Spatial patterns of nitrogen uptake and phytoplankton in the equatorial upwelling zone (110°W–140°W) during 2004 and 2005. *Deep-Sea Research Part II: Topical Studies in Oceanography*, 58(3–4): 417–433
- Paytan A, McLaughlin K. 2007. The oceanic phosphorus cycle. *Chemical Reviews*, 107(2): 563–576, doi: [10.1021/cr0503613](https://doi.org/10.1021/cr0503613)
- Raven J A, Richardson K. 1984. Dinophyte flagella: a cost-benefit analysis. *New Phytologist*, 98(2): 259–276, doi: [10.1111/j.1469-8137.1984.tb02736.x](https://doi.org/10.1111/j.1469-8137.1984.tb02736.x)
- Redfield A C, Ketchum B H, Richards F A. 1963. The influence of organisms on the composition of seawater. In: Hill M N, ed. *The Sea, Vol. 2: The Composition of Sea-Water Comparative and Descriptive Oceanography*, Interscience Publishers. New York: John Wiley, 26–77
- Richardson T L, Gibson C E, Heaney S I. 2000. Temperature, growth and seasonal succession of Phytoplankton in Lake Baikal, Siberia. *Freshwater Biology*, 44(3): 431–440, doi: [10.1046/j.1365-2427.2000.00581.x](https://doi.org/10.1046/j.1365-2427.2000.00581.x)
- Selph K E, Landry M R, Taylor A G, et al. 2011. Spatially-resolved taxon-specific phytoplankton production and grazing dynamics in relation to iron distributions in the Equatorial Pacific between 110 and 140°W. *Deep-Sea Research Part II: Topical Studies in Oceanography*, 58(3–4): 358–377
- Shentu Haigang, Xu Zhihong, Wang Hongfa. 2009. Contrast study to data from geological sampling and deep-tow system of dense portion in China Pioneer Area. *Journal of Marine Sciences*, 27(4): 17–23
- Stoecker D K. 1999. Mixotrophy among Dinoflagellates. *Journal of Eukaryotic Microbiology*, 46(4): 397–401, doi: [10.1111/j.1550-7408.1999.tb04619.x](https://doi.org/10.1111/j.1550-7408.1999.tb04619.x)
- Stramski D, Reynolds R A. 1993. Diel variations in the optical properties of a marine diatom. *Limnology and Oceanography*, 38(7): 1347–1364, doi: [10.4319/lo.1993.38.7.1347](https://doi.org/10.4319/lo.1993.38.7.1347)
- Sun Jun, Liu Dongyan. 2002. The preliminary notion on nomenclature of common phytoplankton in China Seas waters. *Oceanologia et Limnologia Sinica*, 33(3): 271–286
- Sun Jun, Liu Dongyan, Qian Shuben. 2002. A quantitative research and analysis method for marine phytoplankton: an introduction to Utermöhl method and its modification. *Journal of Oceanography of Huanghai & Bohai Seas*, 20(2): 105–112
- Talley L D, Pickard G L, Emery W J, et al. 2011. *Descriptive Physical Oceanography: An Introduction*. Boston: Academic Press
- Tang Senming, Chen Xingqun. 2006. Phytoplankton diel rhythm in the waters of Quanzhou Bay in Fujian, China. *Haiyang Xuebao (in Chinese)*, 28(4): 129–137
- Taylor A G, Landry M R, Selph K E, et al. 2011. Biomass, size structure and depth distributions of the microbial community in the eastern equatorial Pacific. *Deep-Sea Research Part II: Topical Studies in Oceanography*, 58(3–4): 342–357
- Tomas C. 1997. *Identifying Marine Phytoplankton*. San Diego: Academic Press, 1–858
- Tsuchiya M. 1968. *Upper Waters of the Intertropical Pacific Ocean*. Baltimore: Johns Hopkins Press, 1–50
- Turner J W, Good B, Cole D, et al. 2009. Plankton composition and environmental factors contribute to *Vibrio* seasonality. *The ISME Journal*, 3(9): 1082–1092, doi: [10.1038/ismej.2009.50](https://doi.org/10.1038/ismej.2009.50)
- van Haren H, Mills D K, Westeyn L P M J. 1998. Detailed observations of the phytoplankton spring bloom in the stratifying central North Sea. *Journal of Marine Research*, 56(3): 655–680, doi: [10.1357/002224098765213621](https://doi.org/10.1357/002224098765213621)
- Vanreusel A, Hilario A, Ribeiro P A, et al. 2016. Threatened by mining, polymetallic nodules are required to preserve abyssal epifauna. *Scientific Reports*, 6: 26808, doi: [10.1038/srep26808](https://doi.org/10.1038/srep26808)
- Villarino M L, Figueiras F G, Jones K J, et al. 1995. Evidence of *in situ* diel vertical migration of a red-tide microplankton species in Ría de Vigo (NW Spain). *Marine Biology*, 123(3): 607–617, doi: [10.1007/BF00349239](https://doi.org/10.1007/BF00349239)
- Volz J B, Mogollón J M, Geibert W, et al. 2018. Natural spatial variability of depositional conditions, biogeochemical processes and element fluxes in sediments of the eastern Clarion-Clipperton Zone, Pacific Ocean. *Deep-Sea Research Part I: Oceanographic Research Papers*, 140: 159–172, doi: [10.1016/j.dsr.2018.08.006](https://doi.org/10.1016/j.dsr.2018.08.006)
- Wilson G D F. 2017. Macrofauna abundance, species diversity and turnover at three sites in the Clipperton-Clarion Fracture Zone. *Marine Biodiversity*, 47(2): 323–347, doi: [10.1007/s12526-016-0609-8](https://doi.org/10.1007/s12526-016-0609-8)
- Yang Jiaowen, Hua Di, Gu Xingen. 1994. Ecological study on diurnal dynamics of phytoplankton in the pinnate front of the Yangtze River Estuary. *Journal of Marine Sciences*, 12(1): 47–57
- Zeppilli D, Pusceddu A, Trincardi F, et al. 2016. Seafloor heterogeneity influences the biodiversity-ecosystem functioning relationships in the deep sea. *Scientific Reports*, 6: 26352, doi: [10.1038/srep26352](https://doi.org/10.1038/srep26352)
- Zinssmeister C, Wilke T, Hoppenrath M. 2017. Species diversity of dinophysoid dinoflagellates in the Clarion-Clipperton Fracture Zone, eastern Pacific. *Marine Biodiversity*, 47(2): 271–287, doi: [10.1007/s12526-016-0607-x](https://doi.org/10.1007/s12526-016-0607-x)